Available online at www.sciencedirect.com
ScienceDirect
Journal of Molecular Catalysis A: Chemical 268 (2007) 59–64
JOURNAL OF MOLECULAR CATALYSIS A: CHEMICAL
www.elsevier.com/locate/molcata

A simple method for preparing highly active palladium catalysts loaded on various carbon supports for liquid-phase oxidation and hydrogenation reactions

Takashi Harada [a], Shigeru Ikeda [a,*], Mayu Miyazaki [a], Takao Sakata [b], Hirotaro Mori [b], Michio Matsumura [a]

[a] *Research Center for Solar Energy Chemistry, Osaka University, 1-3 Machikaneyama, Toyonaka 560-8531, Japan*
[b] *Research Center for Ultra-High Voltage Electron Microscopy, Osaka University, 7-1 Mihogaoka, Ibaraki 567-0047, Japan*

Received 19 June 2006; received in revised form 1 December 2006; accepted 6 December 2006
Available online 10 December 2006

Abstract

Preparation of nanosized palladium (Pd) catalysts supported on various carbon supports using a simple liquid-phase reduction of aqueous Pd complexes with potassium borohydride (KBH_4) was investigated. We found that addition of appropriate amounts of sodium hydroxide (NaOH) into aqueous solutions of sodium tetrachloropalladate (Na_2PdCl_4) followed by reduction with KBH_4 produced highly dispersed Pd nanoparticles less than 5 nm in diameter on any carbon supports. Ultraviolet–visible light (UV–vis) absorption spectra of aqueous Na_2PdCl_4 solutions in the presence of various amounts of NaOH clarified the occurrence of partial or complete ligand exchange of the Pd complex from chloride ions (Cl^-) to hydroxide ions (OH^-). Hence, the production of small Pd nanoparticles on carbon supports is likely to be induced by structural change in the precursor complex prior to the reduction with KBH_4. Moreover, evaluation of catalytic activities for liquid-phase oxidation of benzyl alcohol into benzaldehyde using oxygen and hydrogenation of the C=C bond in cinnamaldehyde with hydrogen revealed that catalytic functions were significantly dependent on the size and the dispersion of Pd particles; i.e., both reactions proceeded efficiently on small Pd catalysts highly dispersed on carbon supports but did not occur efficiently on Pd particles of relatively large sizes or with poor dispersion on those supports.

Keywords: Palladium nanoparticles; Carbon supports; Effect of sodium hydroxide addition; Liquid-phase catalytic reactions; Ligand exchange

1. Introduction

Pd catalysts supported on carbon materials such as activated carbon (AC) and carbon nanofibers have been extensively employed as catalysts not only for hydrogenation and dehydrogenation in industrial reactions but also for oxidation in the area of fine chemicals [1–4]. Use of these catalysts has many advantages from a practical point of view, e.g., chemical stability, harmlessness, availability of carbon supports, and simplicity of recovery of Pd metal by just burning off carbon components. Moreover, these catalysts are particularly attractive in applications in various kinds of C–C bond formation reactions [5–13] because of their expediency of re-use and sufficient catalytic activities in comparison with homogeneous Pd catalysts such as $Pd(OAc)_2$ [14], *N*-heterocyclic carbene complexes [15], and a triphenylphosphine complex ($Pd(Ph_3P)_4$) [16].

It is well known that the catalytic activity of such Pd-supported carbons strongly depends on the physicochemical properties of Pd particles and carbons, such as size and dispersion of loaded Pd particles, porous structures and surface properties of carbon supports [17]. Hence, effective control of these properties by modifying surface functional groups on carbon supports [18,19] or by the use of carbons with well-controlled nanostructure such as mesoporous carbons [20,21] and carbon nanotubes [22,23] has been studied in order to construct efficient catalytic systems. However, the former requires multiple and/or elaborate preparation steps and the latter represents an incoming research at present.

On the basis of these facts, our interest has been focused on the development of a simple method for controlling size, dispersion, and catalytic functions of Pd nanoparticles on any carbon supports. Among various possible methods, we paid particular

* Corresponding author. Tel.: +81 6 6850 6696; fax: +81 6 6850 6699.
E-mail address: sikeda@chem.es.osaka-u.ac.jp (S. Ikeda).

1381-1169/$ – see front matter © 2006 Elsevier B.V. All rights reserved.
doi:10.1016/j.molcata.2006.12.010

attention to a standard liquid-phase reduction of an aqueous palladium complex as a candidate because of its simplicity and mild operation temperature. We found that addition of an appropriate amount of NaOH to an aqueous solution containing Na_2PdCl_4 followed by reduction with KBH_4 produced highly dispersed Pd nanoparticles with a narrow size distribution on both commercial and synthesized carbon supports. Moreover, thus-obtained Pd nanoparticles on carbon supports were found to exhibit a high level of catalytic activity for liquid-phase oxidation of benzyl alcohol (BA) using molecular oxygen (O_2) and hydrogenation of the C=C bond of cinnamaldehyde (CA) under mild conditions. In this paper, we describe in detail the effects of NaOH addition on structural characteristics and catalytic activity of Pd nanoparticles loaded on some representative carbon supports, carbon black (CB), AC, and a mesoporous carbon (CMK-3) [24].

2. Experimental

2.1. Preparation of catalysts

CB (80 $m^2\ g^{-1}$) and AC (1500 $m^2\ g^{-1}$) were purchased from Wako Pure Chemical and were used as received. CMK-3 (1200 $m^2\ g^{-1}$, 3.3 nm in average pore diameter) was synthesized by using mesoporous silica (SBA-15) as a template [24,25]. Typically, 4 g of SBA-15 (700 $m^2\ g^{-1}$, 6.7 nm in average pore diameter) was added to 0.29 mmol dm^{-3} of aqueous sulfuric acid containing 5 g of sucrose. The slurry was placed in a drying oven at 373 K for 6 h. Then the temperature of the oven was increased to 433 K and maintained at that temperature for 6 h. A brown lump thus-obtained was ground into a powder and was again impregnated with carbon sources by the same treatment. After carbonization of the powder as-obtained at 1173 K under vacuum, the SBA-15 template was removed by soaking in 10 vol% hydrofluoric acid for 3 h followed by repeated washing with distilled water. The structure of thus-obtained CMK-3 was confirmed by powder X-ray diffraction (XRD) and nitrogen adsorption/desorption measurement.

Pd particles loaded on various carbon supports were prepared as follows. 0.2 g of CMK-3, CB, or AC was added to 5 cm^3 distilled water containing NaOH. After agitation of the slurry for a few minutes, 10 cm^3 of aqueous Na_2PdCl_4 solution (10.1 mmol dm^{-3}, corresponding to 5 wt% of Pd) was added dropwise and the mixture was stirred for 48 h at room temperature. Subsequently, 5 cm^3 of aqueous KBH_4 solution was added and the mixture was further stirred for 0.5 h. The resulting suspension was filtered, washed with distilled water several times, and dried at 353 K overnight. Thus-obtained powders of Pd nanoparticles loaded on CMK-3, CB, and AC are labeled Pd/CMK-3, Pd/CB, and Pd/AC, respectively. Note that the amount of NaOH in the solution was varied to study the effect on the structure and catalytic performance of Pd nanoparticles. For a convenient abbreviation of the NaOH content during the above-described procedure, γ, defined as specific molar content of NaOH to that of Na_2PdCl_4 ([NaOH]/[Na_2PdCl_4]) was introduced, and six kinds of samples on each support were prepared with different γ values (γ = 0, 2, 4, 8, 10, and 20).

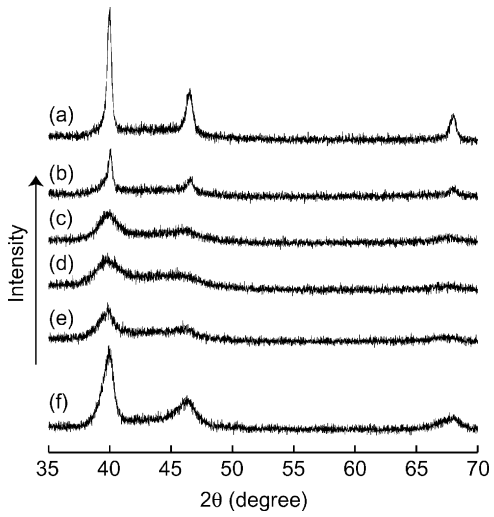

Fig. 1. XRD patterns of Pd/CMK-3 prepared with various NaOH contents: (a) γ = 0, (b) γ = 2, (c) γ = 4, (d) γ = 8, (e) γ = 10, and (f) γ = 20.

2.2. Characterization

XRD patterns were recorded using a Rigaku MiniFlex X-ray diffractometer (Cu Kα, Ni filter). Transmission electron microscope (TEM) images were obtained using a Hitachi H-9000 TEM at a voltage of 300 kV. UV–vis absorption spectra were recorded using a Shimadzu UV-2500PC spectrophotometer.

2.3. Catalytic reactions

Catalytic activities of various Pd-supported carbons were evaluated by liquid-phase oxidation of BA into benzaldehyde (BAH) and liquid-phase hydrogenation of CA into 3-phenylpropionaldehyde (PPA). To a cylindrical reaction vessel (2 cm in diameter) with a reflux condenser, 10 mg of catalyst powder (corresponding to 4.7 μmol of Pd) and 5 cm^3 of 1,4-dioxane were added. For oxidation of BA, 2 mmol of BA was subsequently added, and the heterogeneous reaction mixture was stirred at 353 K under atmospheric pressure of O_2. Hydrogenation of CA was conducted using 1.5 mmol of CA at 303 K under continuous hydrogen (H_2) bubbling (20 $cm^3\ min^{-1}$) through the liquid phase. Amounts of products were determined using a Shimadzu GC2010 gas chromatograph equipped with a flame ionization detector and a TC-FFAP capillary column.

3. Results and discussion

3.1. Characterization of catalysts

Fig. 1 shows XRD patterns of Pd/CMK-3 prepared with various NaOH contents (γ = 0–20). All of the samples exhibited three peaks at 2θ of 40°, 46° and 68°, ascribed, respectively, to (1 1 1), (2 0 0), and (2 2 0) reflections of Pd metal with a face-centered cubic (fcc) structure. Noticeable changes observed in these XRD patterns are their peak width and height depending on the value of γ: a large decrease in peak height accompanied by broadening of width was observed in the case of γ values rang-

ing from 0 to 10, and vice versa at $\gamma = 20$. These results imply that addition of NaOH changes crystallite sizes of loaded Pd nanoparticles. Similar tendencies were also observed on Pd/CB and Pd/AC (data not shown).

For the evaluation of these changes quantitatively, crystallite sizes of Pd particles were calculated from the peak width at half height of the Pd(1 1 1) reflection by applying the Scherrer equation, and results are shown in Fig. 2. Despite significant differences in crystallite sizes ranging from ca. 8 nm (for Pd/CB) to ca. 80 nm (for Pd/AC) without addition of NaOH ($\gamma = 0$), these sizes decreased when NaOH was present in the solution during the synthesis. They were drastically reduced to less than 6 nm in the case of γ values of 4–10 on all carbon supports.

Fig. 3 shows TEM images of Pd/CMK-3 prepared with various NaOH contents. When Pd particles were loaded without NaOH ($\gamma = 0$), Pd particles of various sizes were observed (Fig. 3a). The average particle size was estimated to be 10 nm in diameter. A significant deviation from the crystallite size (25 nm at $\gamma = 0$, see Fig. 2) determined by the above XRD analysis is due to the presence of much larger Pd particles (arrows in Fig. 3a), which probably lead to overestimation of the crystallite size using the Scherrer equation [26]. On the other hand, well-dispersed Pd nanoparticles with a narrow particle-size distribution centered at around 5 nm in diameter were observed at the γ value of 4 (Fig. 3b). This value is consistent with the above-described results of XRD analysis, indicating a single crystalline nature of these nanoparticles. It should be noted that the size of

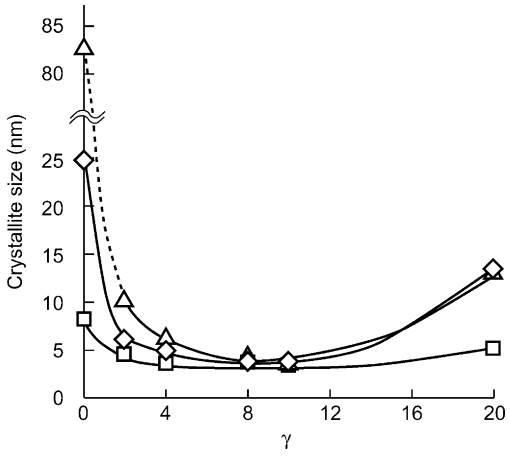

Fig. 2. Plots of crystallite sizes of Pd particles on various carbon supports versus γ value. Diamonds, squares, and triangles denote Pd/CMK-3, Pd/CB, and Pd/AC, respectively.

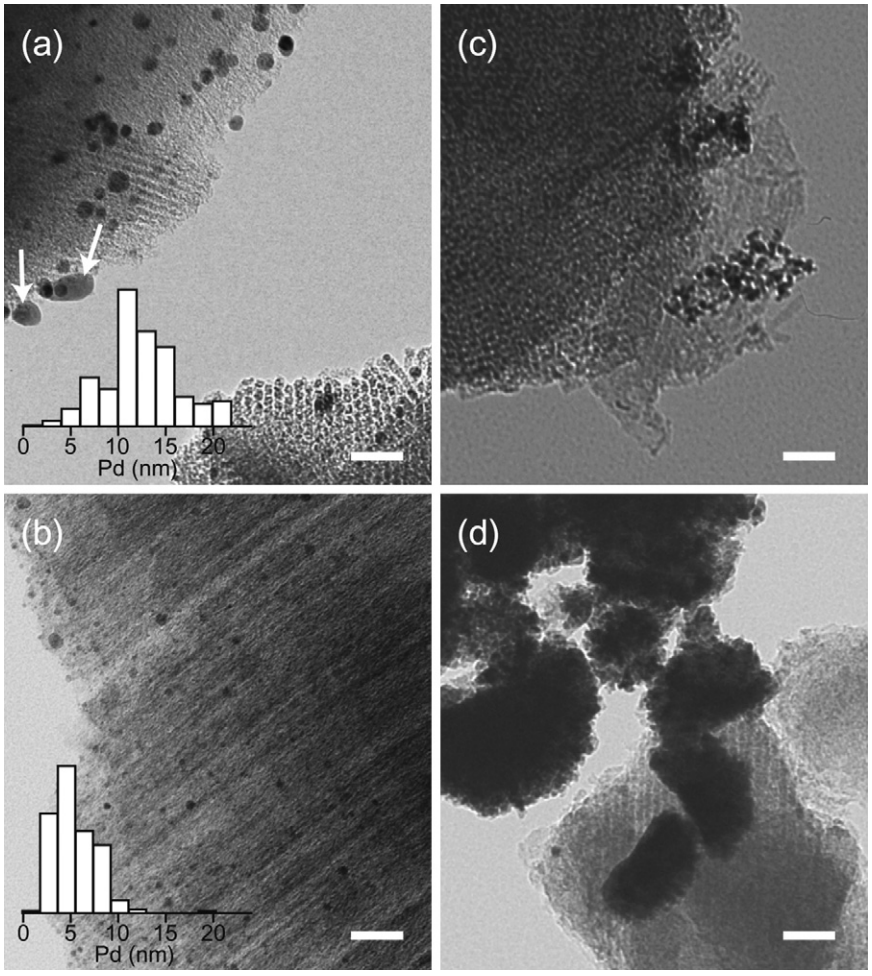

Fig. 3. TEM images of Pd particles supported on CMK-3 prepared with various NaOH contents: (a) $\gamma = 0$, (b) $\gamma = 4$, (c) $\gamma = 10$, and (d) $\gamma = 20$. Scale bars correspond to 50 nm. Insets of figures (a) and (b) represent size distribution of Pd particles determined from TEM images by measuring sizes of more than 200 particles.

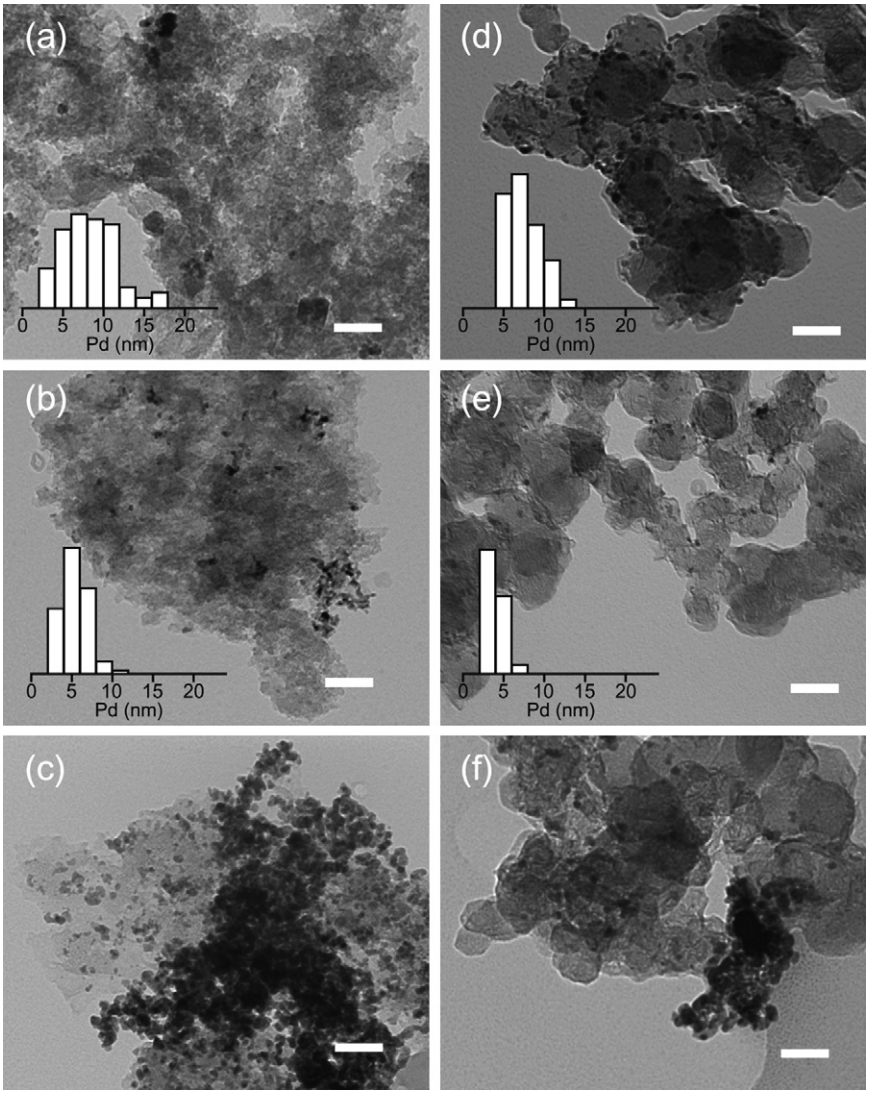

Fig. 4. TEM images of Pd particles supported on AC (a–c) and CB (d–f) prepared at $\gamma = 0$ (a and d), $\gamma = 4$ (b and e), and $\gamma = 20$ (c and f). Scale bars correspond to 50 nm. Particle size distributions of Pd particles are also shown in insets of figures (a), (b), (d), and (e).

these Pd nanoparticles is larger than the pore diameter of CMK-3 used (3.3 nm in average diameter). Thus, Pd particles are distributed on the external surface of CMK-3 rather than inside the pore system of CMK-3. As shown in Fig. 3c, an increase in the NaOH content ($\gamma = 10$) led to poor dispersion of Pd on CMK-3, while the sizes of individual particles seemed to be smaller than the sizes of particles prepared at the γ value of 4 as expected from the results of XRD analysis. Aggregation of particles became intense when the content of NaOH increased to the γ value of 20; production of aggregates of Pd nanoparticles of several hundreds of nanometers in diameter was confirmed from the TEM image shown in Fig. 3d. On AC and CB supports, strikingly similar changes in particle size, size distribution, and dispersibility of Pd particles depending on the NaOH content were observed, as shown in Fig. 4; inhomogeneous sizes and size-distributions of Pd particles at $\gamma = 0$ (Fig. 4a and d) became uniform (5.4 at $\gamma = 4$), and further addition of NaOH ($\gamma = 20$) induced aggregation (Fig. 4c and f). Hence, we clearly demonstrated the controllability of particle sizes and dispersibilities of Pd nanoparticles by just adding appropriate amounts of NaOH regardless of the kind of carbon support.

In order to investigate the above-described structural changes of Pd particles induced by NaOH addition, we tried to identify the structure of Na_2PdCl_4, the precursor of Pd nanoparticles, in the solution in the absence and presence of NaOH by using UV–vis absorption spectroscopy. Representative results are shown in Fig. 5. The spectrum of the sample without NaOH ($\gamma = 0$) exhibits two absorption bands centered at 207 and 237 nm (Fig. 5a). These are assigned to ligand-to-metal charge transfer (LMCT) bands of a $[PdCl_3(H_2O)]^-$ complex [27]. Addition of a small amount of NaOH, corresponding to the γ value of 0.5, induces a decrease in these two absorption bands accompanied by the appearance of a broad absorption band centered at ca. 280 nm, which reached a maximum at the γ value of 1 (Fig. 5b and c). According to the literature [28–30], this absorption band can be assigned to the LMCT band of mixed chlorohydroxypalladium(II) species, e.g., $[PdCl_2(OH)_2]^{2-}$ and $[PdCl_3(OH)]^{2-}$. Other noticeable changes observed in the spectrum ($\gamma = 1$) are

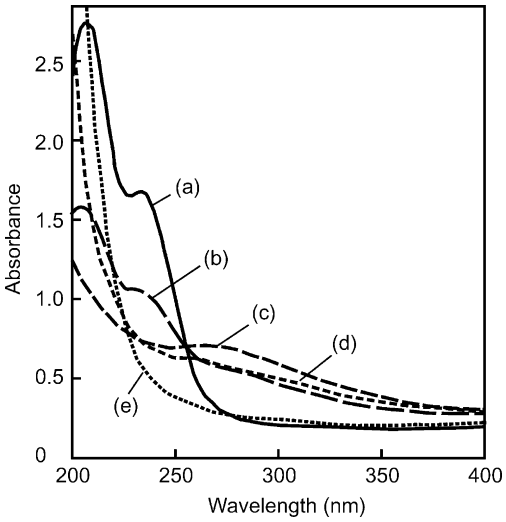

Fig. 5. UV–vis spectra of aqueous Na_2PdCl_4 solutions in the absence and presence of NaOH: (a) $\gamma = 0$, (b) $\gamma = 0.5$, (c) $\gamma = 1$, (d) $\gamma = 4$, and (e) $\gamma = 10$.

disappearance of absorption bands of the $[PdCl_3(H_2O)]^-$ complex and an increment in the background intensity at ca.<240 nm. Since the background intensity increased at a higher content of NaOH ($\gamma > 1$, Fig. 5d and e), this is probably attributed to the scattering induced by the formation of colloidal $Pd(OH)_2$ particles. Actually, visual observation indicated the formation of a colloidal sol in the solution when the content of NaOH was further increased ($\gamma = 20$).

Consequently, addition of NaOH with γ values between 0 and 20 in the present study induced partial or complete ligand exchange of Cl^- for OH^-. The change in particle size from a few tens nm ($\gamma = 0$) to ca. 5 nm ($\gamma \leq 10$) shown by the XRD and TEM results corresponds to such ligand exchange prior to the reduction with KBH_4. Namely, precursor complexes containing OH^- ligand(s) are much more favorable for the formation small Pd nanoparticles on carbon supports than those without an OH^- ligand. On the other hand, due to the formation of $Pd(OH)_2$ particles before the KBH_4 reduction in the presence of a relatively large amount of NaOH ($\gamma \geq 10$), monodispersibility of Pd nanoparticles was reduced by the formation of large aggregates as shown by TEM findings (see Figs. 3 and 4).

3.2. Catalytic activities

Fig. 6 shows catalytic properties of Pd/CMK-3, Pd/CB, and Pd/AC prepared with various contents of NaOH for oxidation of BA using atmospheric pressure of O_2 at 353 K for 1 h, together with those of a commercial carbon-supported Pd catalyst (c-Pd/C, Pd: 5 wt%) supplied by N.E. Chemcat [31]. For Pd/CB samples, conversion of BA for a shorter reaction period (0.5 h) is also shown in the inset of this figure in order to evaluate the dependence on the γ value. All of the catalysts suspended and agitated in 1,4-dioxane containing BA gave BAH with production of other by-products, mainly benzoic acid and benzyl benzoate. No leaching of palladium species into the solvent was confirmed by inductively coupled plasma (ICP) analysis (under the detection limit (<5 ppm)) for some selected samples, indicating that the observed activity is derived from the heterogeneous

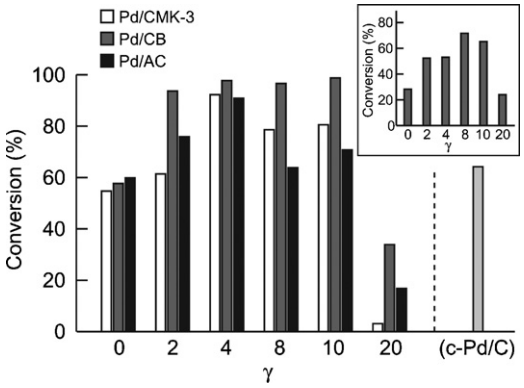

Fig. 6. Oxidation of benzyl alcohol into benzaldehyde by Pd particles loaded on various carbon supports and by a commercial catalyst (c-Pd/C) under atmospheric pressure of O_2 at 353 K for 1 h. Inset shows conversion data obtained on Pd/CB for a shorter period (0.5 h).

catalytic function of present materials. Since the selectivity of the aldehyde production, defined as the percentage of the BAH yield to the total amount of detected products, was ca. 80% on all of the catalysts shown in this figure, we used conversion of BA as a measure of their catalytic performance. On all the catalysts, enhancement of conversion was clearly observed when catalysts prepared by addition of an appropriate amount of NaOH ($2 \leq \gamma \leq 10$) were used. Maximum efficiencies much higher than that of c-Pd/C were achieved on catalysts prepared at the γ value of 4 (CMK-3, AC) or 8 (CB). In accordance with the results of structural analyses described above, such an increase in catalytic activity is mainly due to the small size of Pd nanoparticles, leading to an increment in active sites for the reaction. On the other hand, there are apparent decreases in activity of all of the catalysts prepared at the γ value of 20. As was confirmed by TEM observation (Figs. 3d and 4c,f), this is due to the formation of large aggregates of Pd nanoparticles; a limited number of active sites can be utilized for the catalytic cycle on such aggregates.

Another point worth noting is that the Pd/CB catalyst gave higher conversion than did Pd/CMK-3 and Pd/AC. As described below, a similar trend was also observed in the hydrogenation of CA. Based on the XRD and TEM results, this trend is probably attributable to the relatively small crystallite (particle) size of Pd nanoparticles on CB compared to those on other supports, leading to utilization of relatively large number of active sites.

Table 1 summarizes the results of hydrogenation of CA on Pd/CMK-3 and Pd/AC as well as on the commercial c-Pd/C catalyst. All of the catalysts used in this study showed activity in the production of PPA with 3-phenylpropanol (PPOH), a by-product formed by hydrogenation of both C=C and C=O bonds in CA. PPA obtained by the catalysts prepared without NaOH ($\gamma = 0$) are comparable (Pd/AC) or less than (Pd/CMK-3 and Pd/CB) that obtained by c-Pd/C. On the other hand, the CA conversion of samples prepared in the presence of NaOH ($\gamma = 2$–10) exceeded that of c-Pd/C. It is notable that the conversion reached a maximum at the γ value of around 4 in the same manner as the above-described BA oxidation. Thus, both particle size and dispersion of Pd nanoparticles remarkably affect the conversion in this reaction; i.e., the larger the surface area of Pd particles, the higher the conversion of CA.

Table 1
Hydrogenation of cinnamaldehyde into 3-phenylpropionaldehyde by Pd particles on various carbon supports

Catalyst	γ	Conversion (%)[a]	Selectivity (%)[b]
Pd/CMK-3	0	13	52
	2	56	75
	4	84	78
	8	81	89
	10	81	86
	20	61	69
Pd/CB	0	36	89
	4	>99	95
	20	34	85
Pd/AC	0	53	95
	4	52	90
	20	22	89
c-Pd/C[c]	–	45	92

Catalytic reactions were carried out at 303 K for 3 h with cinnamaldehyde (1.5 mmol), 1,4-dioxane (5 cm^3), and catalyst powder (10 mg, corresponding to 4.7 μmol of Pd) under continuous bubbling with H_2 (20 cm^3 min^{-1}).

[a] Conversion of cinnamaldehyde.

[b] Selectivity for 3-phenylpropionaldehyde production defined as the percentage of the aldehyde yield to the total amount of products.

[c] A commercial catalyst supplied from N.E. Chemcat.

Except for the Pd/CMK-3 catalyst, a high level of selectivity of PPA production was observed regardless of the kind of support or the content of NaOH, suggesting that chemoselectivity for the C=C bond hydrogenation of CA was insensitive to the structure of the Pd catalyst. On the other hand, there is a clear dependence of selectivity on the NaOH content on Pd/CMK-3. In order to obtain information on such peculiar dependence, reactions of PPA and cinnamyl alcohol were performed on Pd/CMK-3 under the same reaction conditions as those used for hydrogenation of CA; the former was not reduced but the latter was smoothly converted to produce PPOH. These results indicate that nonselective reduction of CA to produce PPOH proceeds through the simultaneous hydrogenation of both C=C and C=O bonds or the consecutive reduction, i.e., hydrogenation of the C=O bond followed by that of the C=C. Hence, the dependence of selectivity on the content of NaOH observed on Pd/CMK-3 is likely to be the difference in adsorption mode of CA. That is, selective absorption of the C=C bond in CA occurred on Pd nanoparticles of Pd/CMK-3 catalysts prepared in the presence of a moderate content of NaOH ($2 \leq \gamma \leq 10$), while the accessibility of the C=O bond in the CA molecule to the surface of Pd nanoparticles might be favorable on Pd/CMK-3 catalysts prepared in the absence of NaOH or the presence of large amounts of NaOH ($\gamma = 20$).

4. Conclusion

We have developed a method for synthesizing highly dispersed Pd nanoparticles on various carbon supports. It was confirmed that these materials worked as efficient catalysts for liquid-phase oxidation of benzyl alcohol using O_2 and for C=C bond hydrogenation of cinnamaldehyde with H_2 under mild conditions. It is advantageous that the present catalysts can be prepared by a simple liquid-phase reduction from available sources. Although we have evaluated catalytic functions only using two substrates as model compounds for oxidation and hydrogenation in the present study, these catalysts might have the potential for inducing these reactions of a variety of substrates. Moreover, these catalysts are expected to be applicable to various kinds of reactions for C–C bond formation. Hence, further studies along these lines are now in progress.

Acknowledgements

The authors thank Professors K. Kaneda and T. Hirai (Osaka University) for their stimulating suggestions and discussion. This research was partially supported by a Grant-in-Aid for Young Scientists (A) (No. 16685020) from the Ministry of Education, Culture, Sports, Science and Technology, and Iketani Science and Technology Foundation.

References

[1] E. Auer, A. Freund, J. Pietsch, T. Tacke, Appl. Catal. A 173 (1998) 259.
[2] J. Aumo, S. Oksanen, J.P. Mikkola, T. Salmi, D.Y. Murzin, Ind. Eng. Chem. Res. 44 (2005) 5285.
[3] A. Santos, P. Yustos, T. Cordero, S. Gomis, S. Rodríguez, F. García-Ochoa, Catal. Today 102–103 (2005) 213.
[4] D.S. Cameron, S.J. Cooper, I.L. Dodgson, B. Harrison, J.W. Jenkins, Catal. Today 7 (1990) 113.
[5] S. Venkatraman, C.-J. Li, Org. Lett. 1 (1999) 1133.
[6] L. Bleicher, N.D.P. Cosford, Synlett (1995) 1115.
[7] G.P. Roth, V. Farina, L.S. Liebeskind, E. Peña-Cabrera, Tetrahedron Lett. 36 (1995) 2191.
[8] D.S. Ennis, J. McManus, W. Wood-Kaczmar, J. Richardson, G.E. Smith, A. Carstairs, Org. Process. Res. Dev. 3 (1999) 248.
[9] U.C. Dyer, P.D. Shapland, P.D. Tiffin, Tetrahedron Lett. 42 (2001) 1765.
[10] J.E. Milne, S.L. Buchwald, J. Am. Chem. Soc. 126 (2004) 13028.
[11] A. Hallberg, L. Westfelt, J. Chem. Soc., Perkin Trans. 1 (1984) 933.
[12] M.T. Reetz, J.G. De Vries, Chem. Commun. (2004) 1559.
[13] K.H. Shaughnessy, R.B. DeVasher, Curr. Org. Chem. 9 (2005) 585.
[14] D.D. Kragten, R.A. Van Santen, J.J. Lerou, J. Phys. Chem. A 103 (1999) 80.
[15] L. Jafarpour, S.P. Nolan, Adv. Organomet. Chem. 46 (2001) 181.
[16] J.P. Wolfe, R.A. Singer, B.H. Yang, S.L. Buchwald, J. Am. Chem. Soc. 121 (1999) 9550.
[17] K. Kohler, R.G. Heidenreich, J.G. Krauter, E. Pietsch, J. Chem. A Eur. J 8 (2002) 622.
[18] J. Li, M.J. Vergne, E.D. Mowles, W.H. Zhong, D.M. Hercules, C.M. Lukehart, Carbon 43 (2005) 2883.
[19] Z. Li, W. Yan, S. Dai, Langmuir 21 (2005) 11999.
[20] H. Yang, D. Zhao, J. Mater. Chem. 15 (2005) 1217.
[21] R. Ryoo, S.H. Joo, M. Kruk, M. Jaroniec, Adv. Mater. 13 (2001) 677.
[22] S. Iijima, T. Ichihashi, Nature 354 (1991) 56.
[23] J.L. Bahr, J.M. Tour, J. Mater. Chem. 12 (2002) 1952.
[24] S. Jun, S.H. Joo, R. Ryoo, M. Kruk, M. Jaroniec, Z. Liu, T. Ohsuna, O. Terasaki, J. Am. Chem. Soc. 122 (2000) 10712.
[25] D. Zhao, J. Feng, Q. Huo, N. Melosh, G.H. Fredrickson, B.F. Chmelka, G.D. Stucky, Science 279 (1998) 548.
[26] The large Pd particles gave intense reflections with narrow peak widths at half height. The overestimation of crystallite size should arise from this.
[27] L.I. Elding, L.F. Oisson, J. Phys. Chem. 82 (1978) 69.
[28] C.D. Tait, D.R. Janecky, P.S.Z. Rogers, Geochim. Cosmochim. Acta 55 (1991) 1253.
[29] R.H. Byrne, L.R. Kump, Geochim. Cosmochim. Acta 57 (1993) 1151.
[30] J.M. Middlesworth, S.A. Wood, Geochim. Cosmochim. Acta 63 (1999) 1751.
[31] The c-Pd/C was activated by H_2 reduction at 473 K just before the reaction.